



## Tritium recycling and retention in JET

P. Andrew<sup>a,\*</sup>, D. Brennan<sup>a</sup>, J.P. Coad<sup>a</sup>, J. Ehrenberg<sup>a</sup>, M. Gadeberg<sup>a</sup>,  
A. Gibson<sup>a</sup>, M. Groth<sup>a</sup>, J. How<sup>a</sup>, O.N. Jarvis<sup>a</sup>, H. Jensen<sup>a</sup>, R. Lässer<sup>a</sup>,  
F. Marcus<sup>a</sup>, R. Monk<sup>a</sup>, P. Morgan<sup>a</sup>, J. Orchard<sup>a</sup>, A. Peacock<sup>a</sup>, R. Pearce<sup>a</sup>,  
M. Pick<sup>a</sup>, A. Rossi<sup>a</sup>, B. Schunke<sup>a</sup>, M. Stamp<sup>a</sup>, M. von Hellermann<sup>a</sup>,  
D.L. Hillis<sup>b</sup>, J. Hogan<sup>b</sup>

<sup>a</sup> JET Joint Undertaking, Abingdon, Oxfordshire OX14 3EA, UK

<sup>b</sup> Oak Ridge National Laboratory, Oak Ridge, TN, USA

---

### Abstract

JET's 1997 Deuterium Tritium Experiment (DTE1) allows a detailed study of hydrogenic isotope recycling and retention in a pumped divertor configuration relevant to ITER. There appear to be two distinct forms of retained tritium. (1) A dynamic inventory which controls the fueling behaviour of a single discharge, and in particular determines the isotopic composition. This is shown to be consistent with neutral particle implantation over the whole vessel surface area. (2) A continually growing inventory, which plays a small role in the particle balance of a single discharge, but ultimately dominates the hydrogenic inventory for an experimental campaign comprising thousands of pulses. This will be the dominant retention mechanism in long-pulse devices like ITER. The JET retention scaled-up to ITER proportions suggests that ITER may reach its tritium inventory limit in less than 100 pulses. © 1999 JET Joint Undertaking, published by Elsevier Science B.V. All rights reserved.

*Keywords:* Tritium retention; Wall pumping; JET

---

### 1. Introduction

The hydrogen isotope inventory in the walls of tokamaks is important in two ways. First, the hydrogen isotopes fueling the discharge will exchange with those in the wall weakening the dependence of the plasma isotopic composition on changes in the fueling isotopic composition. This was observed in TFTR [1] where tritium rich beam mixtures were required to obtain 50/50 DT mixtures.

Second, the rate at which the hydrogenic wall inventory grows can become a concern. A large tritium inventory represents a potential safety hazard, for ex-

ample, in the case of a sudden loss of vacuum. Also the efficient consumption of tritium will ultimately be a factor in the economics of a fusion reactor.

In this paper we present results from JET's recent deuterium–tritium experiments, quantifying the dynamic tritium inventory which affects the recycling during a single pulse, and the slow but ultimately dominant build-up of the tritium inventory over the course of the campaign. The results are used to make an estimate of the tritium inventory that could be expected in a next generation tokamak such as ITER.

### 2. Experiment

JET operated with a machine configuration known as the MkIIa divertor between April 1996 and February 1998. Within this campaign there was an extensive deuterium–tritium experiment, May–November 1997,

---

\* Corresponding author. Tel.: +44 1235 46 458; fax: +44 1235 465 373; e-mail: philip.andrew@jet.uk.

known as DTE1 [2]. JET had previously operated with tritium in the 1991 preliminary tritium experiment, PTE [3], but with much smaller quantities of tritium;  $\sim 5$  mg of tritium were injected into the torus during PTE compared to 35 g in DTE1.

The MkIIa is a single null configuration with a divertor geometry more closed to neutrals than the previous MkI divertor [4]. The MkIIa divertor (Fig. 1) comprises carbon/carbon-fiber-composite tiles mounted on a water cooled support structure. The remainder of the first wall is protected with carbon tiles. All surfaces are periodically coated with thin Be films. Active pumping of neutrals during discharges is accomplished with a cryopump mounted behind the support structure. A neutral particle conductance path between the plasma facing surfaces and the divertor cryopump exists in the form of water-cooled louvres at both corners of the divertor. During operation the ambient temperature of the water-cooled components is about  $40^\circ\text{C}$ , while the ambient tile temperature ranges from  $150^\circ\text{C}$  to  $250^\circ\text{C}$ . The remainder of the vessel is at  $320^\circ\text{C}$ .

The pressure and tritium fraction of the neutrals near the divertor cryopump are sampled during a tokamak pulse by a species selective Penning gauge diagnostic [5]. Tritium fractions below 1% could be deduced from the ratio of DT neutron rate and the total neutron rate knowing the relative cross-sections of the DT and DD reactions [6]. These diagnostics were complemented by a variety of different measurements of tritium fraction of both the plasma and the inter-pulse exhaust gas [7].

Throughout the JET operation the rate at which deuterium or tritium is injected can be accurately measured. During and after DTE1, the torus exhaust was tritiated and had to be processed by the active gas handling system (AGHS) [8]. The AGHS delivered a total of 100 g of tritium to the torus (34.4 g) and one of JET's two neutral beam injection systems (65.6 g, of

which 0.6 g were injected into the torus as an energetic neutral beam). The AGHS reprocessed the exhaust gas on a weekly basis yielding a highly accurate measurement of the tritium inventory in the torus. This measurement actually represented the inventory in both the torus and the neutral beam injection system, but during the first two weeks of operation with virtually all the tritium throughput delivered to the neutral beam system, it was clear that the torus contributed over 90% to the tritium retention during the campaign. It was possible to interpolate the inventory at other times using less accurate, but more frequent measurements of the tritium exhaust [9].

All 5 mg of the torus tritium input in the PTE were introduced by neutral beam injection. Furthermore, the AGHS was not used for the PTE, thus, any precise tritium inventory measurement was only possible by surface analysis of in-vessel components [10] and not by gas balance [11].

### 3. Dynamic retention

It has been observed on JET that the amount of deuterium pumped by the walls in a single pulse is of the order of  $4 \times 10^{22}$  D atoms. This seems large when compared to the area over which there is a significant ion flux,  $\leq 10$  m<sup>2</sup>, and the saturation fluence for these ions,  $\sim 3 \times 10^{20}$  D m<sup>-2</sup> assuming 100 eV energy [12], giving only  $< 3 \times 10^{21}$  D atoms. Two possible explanations have been discussed previously to account for this discrepancy: (1) implanted particles are able, during the pulse, to diffuse to depths significantly greater than the implantation depth [13]; (2) a much larger surface area is involved due to neutral fluxes [3,14]. It is difficult to distinguish between these possibilities since neither the depth nor the areal extent of the wall inventory is measured directly during a discharge. It is shown in Section 5 that the number of D atoms codeposited with C during a pulse is  $< 5 \times 10^{21}$ , so that codeposition is not a major contribution to the wall pumping.

Diffusion might be playing a role at the divertor strike points which can reach  $>700^\circ\text{C}$  during a discharge. This could explain why these areas of net erosion have been observed [15] to have D concentrations  $\sim 10\times$  greater than the value expected from implantation. However, these areas amount to  $<10\%$  of the divertor area, and therefore do not offer an explanation for the magnitude of the wall pumping. The remainder of this section will deal with the neutral flux to the wall as a possible mechanism for wall pumping.

To address the role of neutral fluxes during the pulse, the energies and flux densities of neutrals has been calculated using the EIRENE neutral particle simulation code [16]. For these simulations, the total particle recycling coefficient was taken to be unity. The plasma so-

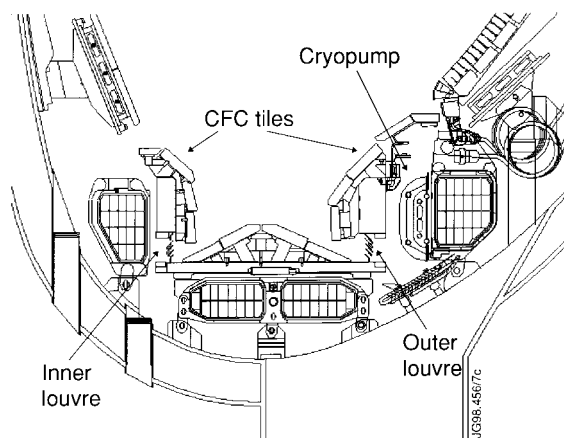


Fig. 1. Cross section of the JET MkIIa divertor.

lution was obtained with the B2 code [17] constrained by Langmuir probe measurements of electron density and temperature as a boundary condition.

The pulse selected for simulation, pulse number 41 677, is the first pulse with significant tritium fueling. The cryopump was off during this pulse. This cryopump condition is not typical; over 90% of the MkIIa campaign was conducted with the cryopump on. However, having the cryopump off does simplify the determination of the wall pumping, and the condition of nearly 100% deuterium in the walls and nearly 100% tritium fueling make this pulse an obvious choice for analysis.

Fig. 2 shows the EIRENE calculation of the neutral flux distribution over the whole vessel surface area. The EIRENE calculation is made for the configuration and Langmuir probe data from  $t=50-60$  s. The flux is largest near the divertor strike points,  $>10^{22} \text{ m}^{-2} \text{ s}^{-1}$ , falling to  $<10^{20} \text{ m}^{-2} \text{ s}^{-1}$  in the top half of the vessel. For comparison, a few available measurements of flux density are shown: divertor neutral flux from ASDEX gauges [18,19], outer midplane pressure measurements assuming a gas temperature of  $320^\circ\text{C}$ , and the inner wall H-alpha light (due to neutral influx to the plasma) assuming 20 ionizations per photon. The data represent the values at  $t=60$  s. The calculated fluxes are everywhere about a factor of 2 higher than the measured fluxes, however the trend, which spans over 2 orders of magnitude is well described. The agreement is reasonable given that the neutral pressures were not used as input constraining the solution.

Fig. 3 shows the measured cumulative wall pumping (i.e., change in wall inventory), determined as the difference between the total fueling and the plasma particle content. This pulse starts in a limiter configuration before becoming a divertor discharge. The total D + T content of the plasma at any time is only a small fraction of the fueling; the majority of the gas is pumped by the walls.

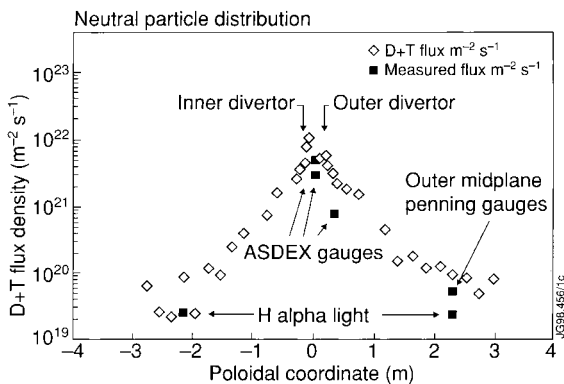


Fig. 2. Poloidal distribution of neutral flux over the vessel surface from EIRENE simulation.

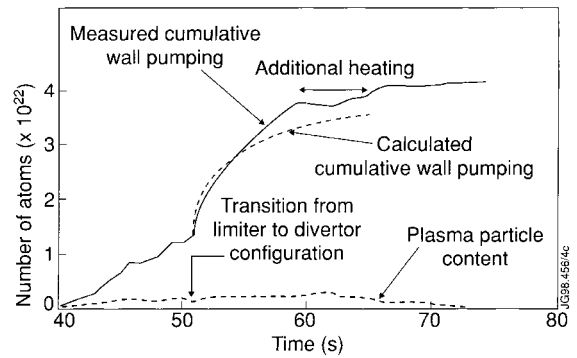


Fig. 3. Wall and plasma inventory during 41 677. Also shown is a calculated change in wall inventory based on the EIRENE fluxes assuming unsaturated surfaces have 0 recycling, and saturated surfaces recycle 100% of the incident flux.

Fig. 3 also shows a calculation of the total wall pumping based on the above neutral flux density distribution for the same pulse. The flux density is taken to be half the EIRENE value for the purposes of the calculation to be consistent with the measured values, and is extrapolated to  $10^{19} \text{ m}^{-2} \text{ s}^{-1}$  at the top of the vessel ( $-4 \text{ m}$  and  $4.5 \text{ m}$  in Fig. 3). Assuming that unsaturated surfaces have a recycling coefficient of 0, and saturated surfaces have a recycling coefficient of unity, the wall pumping is determined as the net fluence to the walls. The initial level of saturation was taken to be 70% to be consistent with the amount of exhaust since the last pulse, assuming it ended with 100% saturation. The saturation concentration for each surface element scales linearly with the EIRENE neutral particle energies, ranging from  $\sim 1.5 \times 10^{22} \text{ m}^{-2}$  close to the divertor where the neutral energy is  $\sim 50 \text{ eV}$ , to  $\sim 6 \times 10^{22} \text{ m}^{-2}$  over most of the main chamber where the neutral energies are of order  $200 \text{ eV}$ . This calculation only considers the divertor phase of the discharge; and is therefore matched to the time and wall inventory corresponding to the start of the divertor phase.

Physically what happens is that areas receiving the largest flux density saturate in  $<15 \text{ ms}$ , and a D saturated region grows during the pulse to include areas of progressively decreasing flux density. The magnitude of the flux density far from the divertor is such that the majority of the whole vessel surface area can be saturated by the end of the discharge.

The agreement is very good considering the following limitations of the calculation.

(1) The calculated neutral flux distribution has been calculated for one time slice, just before the additional heating is switched on. The measured neutral fluxes are observed to rise during the divertor phase, so the calculation would be expected to overestimate the initial rate of wall loading, which it does (Fig. 3).

(2) The calculation is not entirely self consistent. The neutral distribution was calculated for 100% recycling on all surfaces. Clearly if there truly was 100% recycling everywhere, then there would not be any wall pumping. That the neutral fluxes are observed to increase with time is consistent with the fact that the recycling coefficient will also be increasing with time as the surface becomes more and more saturated. This could be addressed by doing a full time dependent and surface-state-dependent simulation.

Fig. 4 illustrates the deuterium and tritium gas balance during the first day of operation with significant tritium fueling. The tritium and total (D and T) fueling to each pulse appears as a step in the cumulative fueling. The exhaust curves are the cumulative exhaust resulting from the inter-pulse outgassing. The exhaust resulting from a test puff of deuterium gas at the start of the day is a rapid and complete recovery of the gas which is introduced. The exhaust after each pulse, however, is a slow incomplete recovery of the total gas with the majority of the tritium input replaced by deuterium exhaust. At the end of the 10 pulse sequence, about 80% of the injected tritium is retained, but the deuterium exhaust greatly exceeds the deuterium input.

The net amount of deuterium recovered in this period gives a lower limit to the wall particle inventory available for isotope exchange. The net amount of deuterium released just prior to the 10th pulse is about  $1.3 \times 10^{23}$  D atoms. This can be compared directly with the saturation fluence used above applied to the whole vessel area:  $6 \times 10^{20} \text{ m}^{-2} \times 200 \text{ m}^2 = 1.2 \times 10^{23}$  atoms. It is also consistent with the total number of traps in the implantation layer,  $1.65 \times 10^{23}$  atoms, deduced from modelling the PTE exhaust [3].

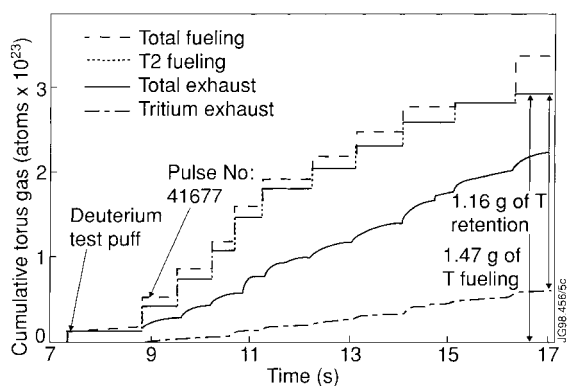


Fig. 4. Cumulative fueling and exhaust for the tritium and total gas during a series of 10 discharges.

#### 4. Long-term retention

In Fig. 4 it is clear that the initial tritium retention is high as a result of tritium replacing previously retained deuterium (isotope exchange), however comparing the total gas input to total exhaust, there is still a deficit, of about 30% retention of the input. When total gas balances are made over an entire day of operation, which includes an overnight period of outgassing, the total gas retention is of order 10% [9]. To analyse the long term tritium retention, we first consider the isotopic fraction during the DTE1.

The tritium fraction during the DTE1 is shown in Fig. 5. The sub-divertor tritium fraction can be resolved down to about 1%. The neutron data assumes that the tritium fraction is equal to 1/300th of the ratio of DT to DD neutron rate. This is a simplification since this factor will depend on whether the neutrons are produced during thermal or beam-plasma reactions. The residual gas analyser measures the exhaust gas tritium fraction between pulses. It was observed that exhaust gas tritium fraction tended to lag behind the plasma tritium fraction. This observation would be expected if the exhaust gas was determined by the wall tritium fraction, but the plasma tritium fraction was determined by both the gas fueling during the pulse and the wall tritium fraction.

Also shown in Fig. 5 is an empirical prediction of the tritium fraction based on the tritium gas input in DTE1, and the observed tritium fraction during the PTE. In the PTE, the tritium exhaust evolution was measured following 5 mg of tritium introduced in two consecutive pulses. Assuming every 5 mg of tritium introduced in

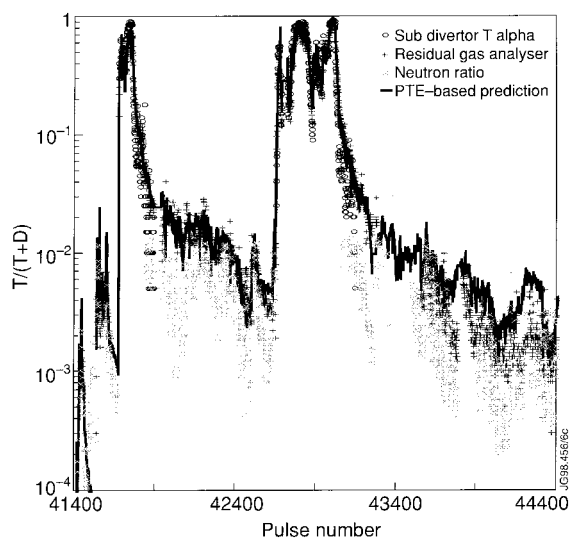


Fig. 5. Tritium fraction measured throughout the DTE by different diagnostics, compared to expectation based on the PTE.

DTE1 makes a similar contribution to the exhaust gas, the DTE1 tritium exhaust can be calculated as a linear sum of PTE-type exhausts. To obtain a tritium fraction, the deuterium exhaust is calculated in a similar fashion.

The tritium fraction in DTE1 is very close to the PTE-based prediction. The DTE1 RGA data follows the prediction better than the two measurements of plasma tritium fraction; this is consistent with the fact that the prediction is based on PTE exhaust measurements. The degree of agreement is surprising given the presence of the divertor cryopump, absent during the PTE. The amount of gas pumped by the cryopump during a pulse often exceeds the amount of wall pumping, and therefore might have been expected to alter the isotope changeover rate. The average gas fueling per pulse increased to  $\sim 5 \times 10^{22}$  atoms in the MkIIa from  $3 \times 10^{22}$  atoms at the time of the PTE. This is due to the cryopump supplementing the wall pumping, and has been modelled in Ref. [20].

The PTE-based prediction of the tritium exhaust per DTE1 pulse can be subtracted from the measured input per pulse to get a prediction of the inventory. This is shown in Fig. 6, together with the measured inventory. The torus inventory measurements are typically accurate to 0.5 g. In contrast to the tritium fraction, the PTE-based prediction does not agree with the measurements. The difference between the measured and predicted inventories increases during the campaign; by the end of the campaign, the measured inventory is over 3× greater than predicted. The tritium inventory at the end of the MkIIa campaign is 6 g, equivalent to 17% of the total tritium input to the torus in DTE1.

Fig. 6 suggests that there is a difference between the way the torus reacts to injected tritium in the MkIIa configuration compared to that at the time of the PTE. This is plausible since the torus was substantially different then. In particular, during the PTE all in-vessel

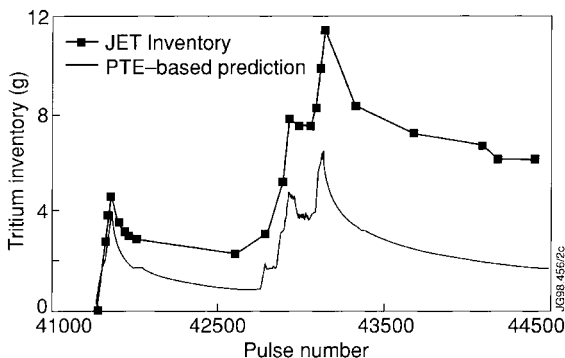


Fig. 6. Tritium inventory in the torus during DTE measured as the difference between the 20 g of tritium on site and the amount measured to be in the AGHS. The expectation based on the PTE is also shown.

surfaces had an ambient temperature of 300°C, and the ‘divertor’ was simply a set of tiles lining the vacuum vessel wall, i.e., an open divertor.

There is also evidence from post-mortem tile analysis that the gas retention is inherently higher in the MkIIa. Analysis of D-rich carbon films made after the first portion of the MkIIa campaign prior to DTE1 [21] revealed quantities of deuterium in the vicinity of the inner MkIIa louvres which exceeded estimates of the total vessel deuterium inventory in campaigns prior to the divertor [22] by a factor of  $\sim 3$ .

To quantify the tritium inventory over and above the PTE-based prediction, the difference between the measured and predicted inventories is shown in Fig. 7. This shows that this difference grows mainly during the periods of tritium fueling, i.e. that the measured and predicted tritium recovery during deuterium pulsing were similar. Also shown in Fig. 7 is the cumulative tritium input to the torus, and the cumulative tritium ion flux to the divertor. The tritium ion flux to the target is not measured directly, but is taken as the product of the plasma tritium fraction (Fig. 5) and the total ion flux to the divertor measured by an array of Langmuir probes. The ion flux determined from Langmuir probes has been cross checked against  $D_2$  light, and is thought to be accurate to better than 50%.

As can be seen from Fig. 7, the difference between measured and predicted tritium inventories grows at a rate which is roughly equivalent to 14% of the cumulative tritium input or alternatively 1.7% of the cumulative T ion flux. A value of 14% of the gas input is consistent with the value of the long-term total gas retention (about 10%).

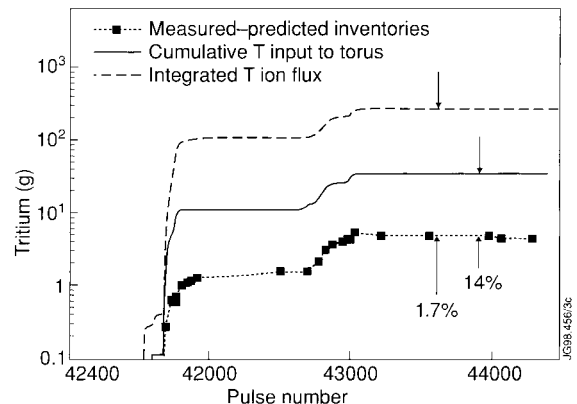


Fig. 7. The difference between measured and predicted inventories growing during the campaign. It grows at a rate which can be expressed as 14% of the gas input or 1.7% of the tritium ion fluence to the divertor.

## 5. Discussion

It is clear that the high levels of tritium retention in DTE1, compared to expectations based on the PTE results, are related to the divertor. Firstly, the cold surfaces in the divertor, such as the louvres, mean that any codeposited films will be saturated with hydrogen isotopes. Post-mortem analysis of films from areas with 300°C ambient temperature show D levels well below the 0.4 D/C found for saturated films [15], a value of  $\sim 0.1$  D/C being typical. However, films with 40°C ambient temperature taken from the MkIIa divertor just prior to DTE1 [21] are found to be saturated with deuterium.

Secondly, the MkIIa divertor comprises regions which see the plasma facing surfaces, but are themselves shadowed from the plasma. This was not the case in the PTE where the divertor target was completely open. Indeed the thick carbon deposits peculiar to the MkIIa are found in precisely these areas [21]. This implies that the gross erosion of carbon could be similar in different divertors, but the substantial shadowed area creates a sink where carbon cannot be re-eroded or heated.

Thirdly, the thickness of redeposited carbon films resulting from a single pulse was estimated to be  $\sim 1.5$  nm for the PTE [3]. It was argued that incoming particles with 8 nm range (100 eV energy) could easily exchange with such an inventory. However, for the thick deposits found in the shadowed regions the film thickness growth per pulse was  $\sim 20$  nm, and the incoming energies would be smaller making most of the trapped inventory inaccessible to release by the incident particle flux.

In Fig. 7, it was shown that the irrecoverable tritium inventory was proportional to about 1.7% of the tritium ion fluence. The post-mortem analysis indicates that the number of carbon atoms deposited in shadowed regions of the inner divertor is 4% of the total ion fluence to the inner target [21], i.e.,  $\sim 5 \times 10^{21}$  carbon atoms per pulse. It was also found that these films, produced at low temperatures by low energy particles had extremely high hydrogenic content. Such high hydrogenic concentration is consistent with the high rate of tritium release observed to emanate from these films during air exposure: over 1 g of T has been recovered from the moisture in the air ventilating the torus during the 1998 remote handling tile exchange [2] which immediately followed the MkIIa campaign. It became clear that during the removal of components from the torus, this unprecedentedly high tritium release rate to the air was due to these films [9]. It was estimated that the deuterium concentration in these films was as high as 0.8 D/C [21].

Given that the inner and outer divertor ion fluences are about balanced during the campaign, and a saturation concentration of 0.8 D/C, this figure would translate to 1.6% codeposited deuterium per total ion fluence, which can be compared directly with the 1.7% figure

above. A proper comparison will be made when the surface analysis of the tritiated films is complete, but from the above results of the pre-DTE1 films, it is clear that the extra inventory in DTE1 relative to the PTE-based expectation can be directly attributed to these D and T rich deposits in the divertor.

In any case, the effective sputtering yield of carbon by ions appears to be a few percent. This is very high, since the gross erosion yield would be expected to be less than 5% [23], and the effective yield less than this due to local redeposition. Furthermore, only a fraction of the eroded carbon would be expected to be deposited in the region of the louvres. This suggests that the mechanism at work is probably not simply erosion by ions.

One possible explanation would be if there was a very large neutral flux to the target, a measure of the neutral flux can be determined from the amount of gas cryopumped during pulses together with the conductance between the target and the pump [24]. The neutral flux to the pumping slots (Fig. 1) estimated this way is about 1/3 the ion flux to the target. Assuming a similar flux over the four tiles surrounding the pumping slots would give a neutral flux about  $2 \times$  greater than the ion flux. The measured and simulated neutral fluxes in the divertor (Fig. 2) suggest a similar magnitude. Neutral fluxes therefore are larger than the ion fluxes, but not by a very large factor.

## 6. Scaling to larger machines

In Sections 3 and 4, the two types of JET tritium retention were quantified: (1) a transiently large dynamic (recoverable) inventory, and (2) a steadily growing irrecoverable inventory. In this section the magnitude of each of these inventories is scaled-up to ITER [25] proportions.

On JET the dynamic inventory is of order  $2 \times 10^{23}$  atoms. It arises from an energy dependent concentration per unit area applicable to the whole vessel area. Taking the ITER area to be  $10 \times$  the JET area, and taking the neutral particle energies to be similar for the two machines gives  $2 \times 10^{24}$  (or 6.7 g of deuterium plus 10 g of tritium). This is about  $10 \times$  smaller than the envisaged fuel requirement per pulse, and about  $100 \times$  smaller than the ITER inventory limit, and therefore not a great concern. From this one does not expect transient wall pumping to be a significant effect well into a 1000 s long ITER discharge.

The long-term retention, however, is a cause for concern. Because the factors determining the gas input pulse (cryopump speeds, neutral pressure at pump inlets and wall pumping capacity) do not necessarily have the same relative importance in JET and ITER, it does not make sense to extrapolate on the basis of tritium gas input.

Instead, the inventory is assumed to grow as 1.7% of the tritium ion flux to the divertor. Although from the discussion of the implied effective yield above, and the observation that there are no deposits on the outer louvres despite a similar ion flux to the outside divertor target, the overall process will be assumed proportional to the ion flux. In JET the total ion fluence to the target is on average  $3 \times 10^{23}$  ions/pulse. For 50/50 DT pulses half this amount would be  $1.7\% \times 1.5 \times 10^{23} = 13$  mg of tritium per pulse. Assuming similar flux density and geometry, this would have to be scaled-up by the ratio of ITER/JET area ( $\sim 10\times$ ) and the ratio of ITER/JET pulse duration in the divertor configuration ( $\sim 100\times$ ). This gives 13 g per ITER pulse. This is a cause for concern since it means the ITER site limit (set at 1 kg for safety reasons) would be reached in less than 100 pulses, i.e., a few days of D–T operation.

A quick check of the simplistic scaling used above can be done by comparing with the TFTR tokamak. The total tritium retention in TFTR [26], a machine with similar size and total discharge time as JET, is of the same order as in JET. Excluding periods of tritium recovery by oxygen cleaning techniques, the cumulative tritium retention in TFTR is the sum of the increase in tritium inventory during the 3 main operating periods, i.e.,  $\sim 1.6 + 1.0 + 0.7 = 3.3$  g [27].

The ITER design has recently included efforts to limit redeposition of carbon to areas with elevated temperatures ( $>500^\circ\text{C}$ ). Such concepts, if successful, could greatly reduce the tritium inventory.

## 7. Summary

On the timescale of one JET pulse the hydrogen (deuterium and tritium) recycling is governed by implantation and isotopic exchange in a thin layer covering the whole vessel surface area. Charge exchange neutrals are the medium by which the flux extends over such a large area. The hydrogenic capacity of this layer is much larger than the amount of hydrogen codeposited in a single pulse. However, in a campaign comprising hundreds of pulses, codeposition will dominate the total hydrogenic inventory.

During the initial period of operation with substantial tritium fueling, the tritium inventory transiently reached 80% of the cumulative tritium fueling. This was the result of isotopic replacement of deuterium in the implantation layer. However, after the end of the tritium campaign the tritium inventory was about 20% of the cumulative fueling, and decreasing only very slowly with subsequent deuterium pulsing.

Such a high, irrecoverable inventory was not expected from our experience with tritium prior to the installation of a divertor in JET. This irrecoverable in-

ventory is associated with codeposition of hydrogen-rich films in the cold and shadowed regions of the JET divertor.

If conditions in ITER are similar to JET, about 13 g of tritium retention can be expected per ITER pulse due to the larger area and longer pulse length. If the rate of carbon erosion cannot be reduced the rate of tritium accumulation could be ameliorated if the redeposition of carbon films could be limited to regions with ambient temperature  $>500^\circ\text{C}$ .

## Acknowledgements

Helpful discussions with Drs L. Horton and G. Matthews are gratefully acknowledged.

## References

- [1] D.K. Owens et al., *J. Nucl. Mater.* 220–222 (1995) 62.
- [2] M. Keilhacker, these Proceedings.
- [3] P. Andrew et al., *Nucl. Fusion* 33 (1993) 1389.
- [4] G.C. Vlases et al., Proceedings of 16th IAEA Conference on Fusion Energy, 1996, p. 371.
- [5] D.L. Hillis et al., *Fus. Eng. Design* 34/35 (1997) 347.
- [6] F.B. Marcus, *Nucl. Fusion* 33 (1993) 1325.
- [7] A. Maas et al., Diagnostic experience during deuterium-tritium experiments in JET, techniques and measurements, to be published in *Fus. Eng. Design*.
- [8] A. Bell, R. Lässer et al., Overview of AGHS operations and performance, to be published in *Fus. Eng. Design*.
- [9] P. Andrew et al., Tritium clean up in JET during and after DTE1, to be published in *Fus. Eng. Design*.
- [10] A.T. Peacock et al., in: *Fusion Technology, Proc. 17th Symp. Rome, 1992*, vol. 1, Elsevier, Amsterdam, 1993, p. 329.
- [11] P. Andrew et al., *J. Nucl. Mater.* 196–198 (1992) 143.
- [12] G. Staudenmaier et al., *J. Nucl. Mater.* 84 (1979) 149.
- [13] J. Ehrenberg et al., *J. Nucl. Mater.* 176–177 (1990) 226.
- [14] P. Andrew, M. Pick, *J. Nucl. Mater.* 220–222 (1995) 601.
- [15] J.P. Coad, M. Rubel, C.H. Wu, *J. Nucl. Mater.* 241–243 (1997) 408.
- [16] D. Reiter et al., *J. Nucl. Mater.* 220–222 (1995) 987.
- [17] R.R. Weynants, G. Van Oost, *Plasma Phys. Contr. Fus* 35B (1993) 177.
- [18] J. Ehrenberg et al., *J. Nucl. Mater.* 241–243 (1997) 420.
- [19] G. Haas et al., *J. Nucl. Mater.* 121 (1984) 151.
- [20] A. Rossi et al., these Proceedings.
- [21] A.T. Peacock et al., these Proceedings.
- [22] J.P. Coad, *J. Nucl. Mater.* 226 (1995) 156.
- [23] B.V. Mech et al., *J. Nucl. Mater.* 241–243 (1997) 1147.
- [24] H. Altmann, P. Andrew, Symposium on Fusion Engineering, San Diego, USA, 1997.
- [25] G. Federici et al., these Proceedings.
- [26] C. Skinner, *J. Nucl. Mater.* 241–243 (1997) 214.
- [27] Nagi et al., 97 Symposium on Fusion Engineering, San Diego, USA, 1997.